Int J Ophthalmol, Vol. 19, No. 7, Jul. 18, 2026 www.ijo.cn
Tel: 8629-82245172 8629-82210956 Email: ijopress@163.com

· Basic Research ·

Metagenomic analysis of ocular microbiome in aqueous humor from myopia, cataract, primary open angle glaucoma and Posner-Schlossman syndrome

Wei-Jia Zhang[1,2,3], *Zhen Yang*[1], *Jian-Qi She*[4,5], *Hong-Ling Wu*[2,3], *Zi-Yao Xia*[2,3], *Di Zhang*[2,3], *Ling-Ge Suo*[1], *Zhe Pan*[2,3], *Yu Zhang*[1], *Huai-Zhou Wang*[2,3], *Jing Hong*[1], *Chun Zhang*[2,3]

[1]Department of Ophthalmology, Peking University Third Hospital, Beijing 100191, China
[2]Beijing Tsinghua Changgung Hospital Eye Center, School of Clinical Medicine, Tsinghua Medicine, Tsinghua University, Beijing 102218, China
[3]Beijing Visual Science and Translational Eye Research Institute (BERI), Beijing 102218, China
[4]Department of Microbiology & Infectious Disease Center, School of Basic Medical Sciences, Peking University Health Science Center, Beijing 100191, China
[5]Department of Radiation Medicine, School of Basic Medical Sciences, Peking University Health Science Center, Beijing 100191, China

Co-first Authors: Wei-Jia Zhang and Zhen Yang

Correspondence to: Chun Zhang and Huai-Zhou Wang. Beijing Tsinghua Changgung Hospital Eye Center, School of Clinical Medicine, Tsinghua Medicine, Tsinghua University, No.168 Litang Road, Changping District, Beijing 102218, China. zhangc1@yahoo.com; trhz_wang@163.com; Jing Hong. Department of Ophthalmology, Peking University Third Hospital, Peking University Eye Center, No.49, North Garden Street, Haidian District, Beijing 100191, China. hongjing1964@sina.com

Received: 2026-02-11 Accepted: 2026-04-03

Abstract

● **AIM:** To characterize the composition and functional features of the aqueous humor microbiome in common ocular diseases, including myopia, cataract, primary open angle glaucoma (POAG), and Posner-Schlossman syndrome (PSS).

● **METHODS:** We performed metagenomic sequencing on 176 aqueous humor samples from patients with cataract (n=37), POAG (n=66), PSS (n=35), and myopia patients (n=38, as controls). Taxonomic profiling, functional annotation, and diversity analyses were conducted to characterize microbial communities, with adjustments for age and gender where appropriate. Associations between microbial features and clinical parameters were evaluated using correlation analyses.

● **RESULTS:** We identified 6635 bacterial, 141 archaeal, 96 eukaryotic, and 108 viral operational taxonomic units (OTUs) in the aqueous humor. The microbiome was dominated by *Actinomycetota* and *Pseudomonadota* at the phylum level. Compared to myopia controls, POAG and PSS patients showed significantly reduced alpha diversity after age adjustment ($P<0.05$), whereas cataract patients showed no significant difference. Additionally, we identified disease-specific microbial signatures including enrichment of *Cytomegalovirus* (CMV) in PSS. Functional analysis revealed enrichment of distinct metabolic pathways. Finally, correlations were observed between microbiota/pathway abundance and clinical phenotype, though none remained significant after multiple testing correction.

● **CONCLUSION:** This study provides a preliminary characterization of the aqueous humor microbiome in patients with POAG, PSS, cataract, and myopia controls. The identified microbial signatures and functional pathways offer new insights into potential microbiome-mediated mechanisms in ocular pathophysiology and may inform future diagnostic and therapeutic strategies.

● **KEYWORDS:** microbiome; aqueous humor; primary open angle glaucoma; Posner-Schlossman syndrome; cataract

DOI:10.18240/ijo.2026.07.03

Citation: Zhang WJ, Yang Z, She JQ, Wu HL, Xia ZY, Zhang D, Suo LG, Pan Z, Zhang Y, Wang HZ, Hong J, Zhang C. Metagenomic analysis of ocular microbiome in aqueous humor from myopia, cataract, primary open angle glaucoma and Posner-Schlossman syndrome. *Int J Ophthalmol* 2026;19(7):1235-1248

INTRODUCTION

The human microbiome plays a pivotal role in maintaining physiological homeostasis and influencing disease pathogenesis across various organ systems, including the eye[1-2]. Traditionally, the intraocular environment, particularly the aqueous humor, was presumed to be sterile due to the closed anatomical structure of the eye and the protection provided by the blood-retinal barrier and blood-aqueous barrier. This view held that any microorganisms detected were considered exogenous pathogens. Therefore, the knowledge of the intraocular microbiome and its function is limited. However, emerging evidence has revealed the presence of microbial communities in intraocular fluids even in the absence of overt infection[3-4]. A systematic study demonstrated the existence of a low-biomass intraocular microbiome in both healthy and diseased human eyes, underscoring the potential for microbial translocation from other body sites, such as the gut, oral, or ocular surface to the intraocular space[4]. These findings have profound implications for understanding ocular health and disease, suggesting that the intraocular microbiome may contribute to both physiological and pathological processes.

Despite these advances, the composition, diversity, and functional dynamics of the aqueous humor microbiome in common ocular diseases, such as myopia, cataract, primary open angle glaucoma (POAG), and Posner-Schlossman syndrome (PSS), remain poorly characterized. POAG is a group of eye disorders characterized by progressive deterioration of the optic nerve that can lead to irreversible vision loss[5]. Although the pathogenesis of POAG is still unclear, previous studies have showed that POAG is related with immune microenvironment disorder[6-7], and *H. pylori* was found in iris specimens of POAG patients[8]. PSS, often linked to cytomegalovirus (CMV) infection, may also involve microbial contributions to immune dysregulation or intraocular pressure (IOP) modulation[9]. This evidence suggested that the microbiome may play an important role in regulating the immune microenvironment and in disease pathogenesis. However, systematic investigations into the aqueous humor microbiome across different ages, sex, and health/disease states are lacking, leaving a critical gap in our understanding of its underlying mechanisms.

Metagenomic sequencing offers a powerful, unbiased approach to profile microbial communities in low-biomass environments like the aqueous humor[10-11]. Unlike traditional culture-based methods that fail to detect unculturable or fastidious microorganisms, metagenomics provides a comprehensive view of microbial diversity by directly sequencing all genetic material in a sample. Although results could also be complicated by several factors, such as small sample size[12], swabbing technique[13], and contamination from DNA extraction and profiling tool[14-15], metagenomics remains the best state-of-the-art tool for *in situ* profiling of a microbiota. This high-throughput technique also enables functional annotation of microbial genes, revealing potential metabolic pathways that may interact with host physiology.

In this work, we performed metagenomic sequencing to investigate the taxonomic and functional landscape of the aqueous humor microbiome in cataract, POAG, and PSS patients compared to young myopia patients as controls. We analyzed aqueous humor specimens obtained during surgery from patients with cataract, POAG, and PSS (with PSS samples collected during an acute episode), as well as from young myopia patients undergoing implantable collamer lens (ICL) surgery, who served as controls. Our findings may contribute to the understanding of microbial contributions to different eye diseases and could offer potential insights into novel biomarkers or therapeutic targets, paving the way for future mechanistic and translational research in ocular health.

PARTICIPANTS AND METHODS

Ethical Approval All samples in this study were obtained from routine clinical practice at Peking University Third Hospital, Peking University. Written informed consent was obtained from all participating patients, which specifically authorized the use of their aqueous humor samples for metagenomic sequencing and the subsequent analysis and publication of the resulting data. The study protocol was reviewed and approved by the Peking University Third Hospital Medical Science Research Ethics Committee (Approval IRB00006761-M2023710), and all procedures were conducted in strict accordance with the ethical principles outlined in the Declaration of Helsinki. This study was registered under the Chinese Clinical Trials Registry (ChiCTR2400090540). The original data was registered under the National Center for Biotechnology Information (PRJNA1187273). To ensure patient privacy, all sequencing reads were subjected to a rigorous bioinformatic filtering step to remove human genetic material prior to any microbial analysis.

Subject Recruitment This study included a total of 176 aqueous humor samples collected at Peking University Third Hospital between December 2023 and December 2024: 37 from cataract patients, 66 from POAG patients, 35 from PSS patients, and 38 from myopia patients. Adult patients who were diagnosed as POAG, PSS, and cataract, who needed surgical treatment and were willing to join the project were enrolled in the study. Besides, we enrolled myopia patients who were willing to undergo ICL surgery as controls due to the difficulty in obtaining aqueous humor from healthy individuals. The inclusion and exclusion criteria for all participants are shown in Table 1.

All enrolled patients underwent a standardized ophthalmic examination, including assessment of visual acuity and IOP, slit-lamp biomicroscopy, gonioscopy, and optic disc evaluation with a 90-diopter (D) lens. Retinal nerve fiber layer (RNFL) was measured by optical coherence tomography (OCT;

Table 1 Inclusion and exclusion criteria

Criteria
Inclusion criteria
Patients aged 18–80y, clearly diagnosed with PSS based on the following clinical characteristics
Recurrent attacks of unilateral elevated IOP in association with mild nongranulomatous anterior uveitis, and attacks last few hours to few weeks
Patients usually complain of decreased vision, mild discomfort, and halos
Corneal edema, elevated IOP, open angle, KPs, few cells, and minimal flare are usually seen in the affected eye
Normal visual fields and optic disc, and normal IOP between attacks
Patients aged 18–80y, clearly diagnosed with POAG based on the following clinical characteristics
Persistent or worsening findings of a 0.3 or greater cup-to-disc ratio
Increasing IOP greater than 21 mm Hg
Nerve fiber layer defects verified with optical coherence tomography
Reproducible visual field defects
Myopia patients aged 18–80y who underwent ICL surgery
Age-related (senile) cataract patients who underwent cataract surgery
Able to understand and willing to sign the informed consent form
Exclusion criteria
Had taken glucocorticoids or immunosuppressive medication within the 3mo prior to sample collection
Elevated IOP caused by any other known factor
Presence or history of eye diseases other than refractive errors
History of ocular trauma, infectious uveitis, other types of immune-related uveitis, or comorbid POAG
History of ophthalmologic surgery or operation, including paracentesis of the anterior chamber
History of uncontrolled systemic diseases known to significantly impact immune function or microbiome, including but not limited to: diabetes mellitus, autoimmune diseases, active cancer and uncontrolled hypertension, or heart disease posing significant peri-procedural risk
Pregnant (including the possibility) or lactating women

PSS: Posner-Schlossman syndrome; IOP: Intraocular pressure; KP: Keratic precipitates; POAG: Primary open angle glaucoma; ICL: Implantable collamer lens.

Heidelberg Engineering, Heidelberg, Germany) and Humphrey visual field (VF) examination (Carl Zeiss Meditec, Dublin, CA, USA) were also performed in the POAG and PSS group. The absence of detailed refractive error data, particularly for the myopia control (MC) group, is a limitation of this study. Future investigations should include comprehensive refractive assessments to better characterize the relationship between myopic status and the intraocular microbiome.

Collection of Aqueous Humor Samples Aqueous humor samples were collected as follows. A topical antimicrobial drug, 0.5% levofloxacin eye drops (Cravit, Santen Pharmaceutical Co., Japan), was administered four times a day in the eye for at least 3d before surgery. On the day of surgery, patients received conjunctival sac irrigation using 0.9% sodium chloride solution at least twice and mydriasis using compound tropicamide eye drops. Following disinfection and draping, 5% povidone-iodine (PVI) was applied to the eye for 30 s. The conjunctival sac was then irrigated with 0.9% sodium chloride solution at least three times. After topical anesthesia with 0.5% alcaine (at least three times), an auxiliary incision was made *via* a 1.5 mm stab knife (Alcon, USA) at the 2 o'clock position of the limbus. The aqueous humor was sampled *via* the auxiliary incision using a 1 mL sterile syringe before any other procedures were initiated. Immediately after collection, aqueous humor samples were transferred into sterile Eppendorf tubes and stored at -80 °C prior to metagenomic next-generation sequencing (mNGS) examination.

Background Contamination Monitoring To systematically assess potential contamination from environmental sources and reagents in our low-biomass metagenomic analysis, we incorporated two categories of negative controls. The first set consisted of conjunctival sac irrigation fluid samples (n=5) collected following routine PVI disinfection, which served to evaluate background microbial signals from the surgical field. The second set comprised balanced saline solution samples (n=5) obtained from sterile, unopened vials used during surgery, allowing us to monitor contamination introduced by reagents or consumables. All control samples were subjected to identical DNA extraction, library preparation, and sequencing workflows as the aqueous humor samples from patients.

DNA Extraction and Sequencing DNA extraction from aqueous humor was performed using the Matridx Biological DNA extraction Kit, according to the manufacturer's instructions. The DNA concentration was estimated by NanoDrop (Thermo Scientific, USA). Metagenomic sequencing libraries were constructed from extracted

DNA and sequenced on the Illumina HiSeq2500 platform. Unlike 16S rRNA gene amplicon sequencing, which targets specific hypervariable regions (*e.g.*, V4 or V5), our shotgun metagenomic approach captures all microbial genetic material, enabling comprehensive taxonomic and functional profiling across bacteria, archaea, viruses, and eukaryotes.

Metagenomic Data Analysis Our study performed metagenomic data analysis based on EasyMetagenome pipeline[16]. Briefly, sequencing reads were firstly quality-assessed by FastQC v0.12.1 (https://www.bioinformatics.babraham.ac.uk/projects/fastqc/) and quality-controlled by fastp v0.24.0[17]. Then, the human-derived sequencing reads were removed with KneadData v0.12.0 (https://huttenhower.sph.harvard.edu/kneaddata) to obtain clean microbiome reads, by mapping human reads to human reference genome (GRCh37) with Bowtie2 v2.5.1[18]. To protect patient privacy, all subsequent microbiome analyses were performed on this filtered, non-human dataset. Taxonomic classification was carried out using Kraken2 v2.1.3[19], while species abundance was estimated with Bracken v2.7[20]. Gene family and pathway relative abundance was calculated with HUMAnN3 v3.7[21]. Linear discriminant analysis (LDA) Effect Size (LefSe 1.0)[22] was applied to identify species and functional pathways characterizing the differences among sample groups with thresholds of LDA Score ≥2 and *P*<0.05. For alpha diversity analysis, we calculated indices such as Richness, Chao1, abundance-based coverage estimator (ACE), and Shannon with "otutab_rare.R", and visualized the results as boxplots using "alpha_boxplot.R" from EasyAmplicon[23]. ANOVA followed by Tukey's honestly significant difference (HSD) test was applied to assess the significance of differences and determine the *P*-value. For beta diversity analysis, we calculated Bray-Curtis metrics with "usearch" and visualized the results as principal coordinate analysis (PCoA) plots using "beta_pcoa.R".

Statistical Analysis All statistical analyses were performed using R software (version 4.1.0; R Foundation for Statistical Computing, Vienna, Austria). For demographic and clinical characteristics, categorical variables like gender were compared using Fisher's exact test or the Chi-square test, as appropriate. Continuous variables [IOP, glaucoma medications, the cup-disc ratio (CDR), RNFL, visual field mean defect (VF-MD) and best-corrected visual acuity (BCVA)] were first assessed for normality using the Shapiro-Wilk test. As most variables were not normally distributed, data are presented as median with interquartile range (IQR), and group comparisons were performed using the Kruskal-Wallis test.

For alpha diversity indices (Richness, Chao1, ACE, Shannon), analysis of covariance (ANCOVA) followed by Tukey's HSD test was applied to assess differences among groups. Beta diversity was evaluated using PCoA based on Bray-Curtis distances, with permutational multivariate analysis of variance (PERMANOVA) used to test for significant differences in community structure between groups.

Differential abundance analysis of microbial taxa and functional pathways was performed using LDA effect size (LEfSe) with thresholds of LDA score ≥2 and *P*<0.05. Correlations between microbial features (genus-level abundance, pathway abundance) and clinical parameters were assessed using Spearman's rank correlation coefficient. To control for multiple testing, we applied the Benjamini-Hochberg false discovery rate (FDR) correction where appropriate. All tests were two-tailed, and *P*<0.05 was considered statistically significant, unless otherwise specified.

RESULTS

Participant Characteristics To systematically investigate the ocular microbiome of the aqueous humor, we collected 176 specimens from eyes in patients with cataract (CAT, *n*=37), POAG (*n*=66), and PSS (*n*=35), as well as myopia patients who underwent ICL surgery (*n*=38). None of the participants had a history of ocular or systemic diseases known to significantly impact immune function or the microbiome, such as infections or inflammatory conditions. The demographic and ophthalmic characteristics of all participants were presented in Table 2. As expected, cataract patients were significantly older than POAG patients, PSS patients and MCs, while patients with POAG and PSS had significantly higher IOP than cataract patients and MCs (all *P*<0.01).

Evaluation of Background Contamination To assess potential contamination, two types of negative controls including conjunctival sac irrigation fluid and balanced saline solution were sequenced in parallel with the aqueous humor samples. Metagenomic analysis of these controls revealed a low-biomass microbial profile, with only two bacterial genera, GGB7511 and *Aquabacterium*, detected in a subset of samples. Importantly, neither genus was found among the dominant taxa (*e.g.*, top 10 most abundant genera) in any patient or control aqueous humor sample. This finding indicates that the primary microbial signals observed are unlikely to originate from procedural or reagent contamination and instead represent genuine biological features of the aqueous humor.

Landscape of Ocular Microbiome in Aqueous Humor After metagenomic sequencing and quality control, we obtained an average of over 4.5 million high-quality clean reads from 176 samples. Using Kneaddata, we eliminated host contamination and retained over 95% sequencing reads for taxonomic assignment and function annotation. By taxonomic profiling and species annotation, we identified a total of 6635 bacteria, 141 archaea, 96 eukaryotes, and 108 viruses in the aqueous humor from the four groups. At the phylum level, *Actinomycetota*, *Pseudomonadota*, *Chordata*, *Bacillota*,

Table 2 Demographics and other characteristics of participants *n* (%) or median (IQR)

Demographics	MC	CAT	POAG	PSS	*P*
Gender					<0.001
Male	13 (34.2)	9 (24.3)	54 (81.8)	25 (71.4)	
Female	25 (65.8)	28 (75.7)	12 (18.2)	10 (28.6)	
Age, y	27.00 (25.00, 32.75)	60.00 (55.00, 66.00)	35.50 (26.00, 43.00)	41.00 (35.00, 49.50)	<0.001
IOP, mm Hg	13.40 (12.30, 14.70)	16.00 (15.00, 17.00)	22.70 (18.00, 27.00)	40.00 (26.25, 45.50)	<0.001
CDR	0.40 (0.30, 0.50)	0.40 (0.30, 0.50)	0.90 (0.80, 0.90)	0.60 (0.40, 0.80)	<0.001
RNFL, µm	-	-	58.00 (54.50, 69.00)	82.00 (64.00, 91.50)	<0.001
VF-MD, dB	-	-	-18.23 (-25.16, -7.70)	-5.00 (-8.01, -1.80)	<0.001
No. of medications	-	-	3.00 (3.00, 4.00)	3.00 (2.00, 3.00)	0.012
CEC, cells/mm^2	-	2797.00 (2531.00, 3026.00)	2698.00 (2531.25, 2817.00)	-	0.268
CCT, µm	-	-	535.00 (520.50, 547.00)	-	-
AXL, mm	26.40 (25.32, 27.07)	23.63 (22.50, 24.91)	25.99 (24.85, 27.35)	-	<0.001
BCVA, logMAR	0.10 (0.00, 0.22)	0.40 (0.22, 0.60)	0.15 (0.00, 0.61)	0.10 (0.00, 0.30)	<0.001

MC: Myopia control; CAT: Cataract; POAG: Primary open angle glaucoma; PSS: Posner-Schlossman syndrome; IOP: Intraocular pressure; CDR: Cup-disc ratio; RNFL: Retinal nerve fiber layer; VF-MD: Visual field mean defect; CEC: Corneal endothelial cells; CCT: Central corneal thickness; AXL: Axial length; BCVA: Best-corrected visual acuity; logMAR: Logarithm of the minimum angle of resolution; IQR: Interquartile range.

and *Mycoplasmatota* were the dominant phyla, accounting for more than 95% of the total abundance (Figure 1A). The relative abundance of *Actinomycetota* in MCs was significantly lower than that in the cataract, POAG, and PSS patients, while the relative abundance of *Pseudomonadota* was significantly higher (all $P<0.01$). Similarly, *Paeniglutamicibacter* at the genus level and *Paeniglutamicibacter sp. ZC-3* at the species level were preponderant in all groups, especially in the cataract, POAG and PSS patients (Figure 1B and 1C). Moreover, *Pseudomonas*, *Ralstonia*, and *Herbaspirillum* were the dominant genera in MCs with significantly higher abundance than in cataract, POAG, and PSS patients (all $P<0.01$). Based on the relative abundance of operational taxonomic units (OTUs), the top 100 species were shown in phylogenetic trees and were mostly enriched in *Pseudomonadota* and *Actinomycetota* (Figure 1D).

Among 6980 OTUs detected in the aqueous humor, almost 50% (n=3414) were shared among MCs and cataract, POAG and PSS patients (Figure 2A). The number of annotated species and unique species in the aqueous humor from PSS patients was the lowest. PCoA showed that the beta diversity of the microbiota was similar among cataract, POAG, and PSS patients (Figure 2B). For MCs, the samples clustered into two subgroups: one with a community structure similar to the patient groups, and another with a distinct structure. To assess the potential confounding effects of age and gender on microbial community structure, we performed PERMANOVA with these variables as covariates. After adjustment, significant differences among the four groups remained (overall PERMANOVA: Group R^2=0.038, P=0.012), while age (R^2=0.0043, P=0.541) and gender (R^2=0.0036, P=0.622) showed no significant effects (Table 3). Pairwise comparisons with FDR correction confirmed that both PSS (PSS *vs* MC: R^2=0.055, adjusted P=0.012) and POAG (MC *vs* POAG: R^2=0.043, adjusted P=0.024) differed significantly from controls, while cataract showed no significant difference from controls after adjustment (MC *vs* CAT: R^2=0.015, P=0.302; Table 3). Additionally, no significant differences were observed among the three disease groups (all $P>0.05$).

Table 3 PERMANOVA results assessing the effects of age, gender, and disease group on microbial community structure

Comparison	Variable	R^2	*F*	*P*	Adjusted *P*
Overall	Age	0.0043	0.785	0.541	-
	Gender	0.0036	0.653	0.622	-
	Group	0.038	2.317	0.012	-
Pairwise comparisons					
PSS *vs* MC	Group	0.055	4.207	0.002	0.012
PSS *vs* POAG	Group	0.010	1.004	0.380	1
PSS *vs* CAT	Group	0.016	1.098	0.350	1
MC *vs* POAG	Group	0.043	4.646	0.004	0.024
MC *vs* CAT	Group	0.015	1.171	0.302	1
POAG *vs* CAT	Group	0.0078	0.808	0.487	1

PERMANOVA: Permutational multivariate analysis of variance; MC: Myopia control; CAT: Cataract; POAG: Primary open angle glaucoma; PSS: Posner-Schlossman syndrome.

Interestingly, alpha diversity was also similar among cataract, POAG, and PSS patients, but significantly lower than that of MCs, suggesting the higher richness and evenness of species in normal aqueous humor (Figure 2C–2F). To control for potential confounding by age and gender, we performed ANCOVA with these variables as covariates. After adjustment, significant differences in alpha diversity among groups

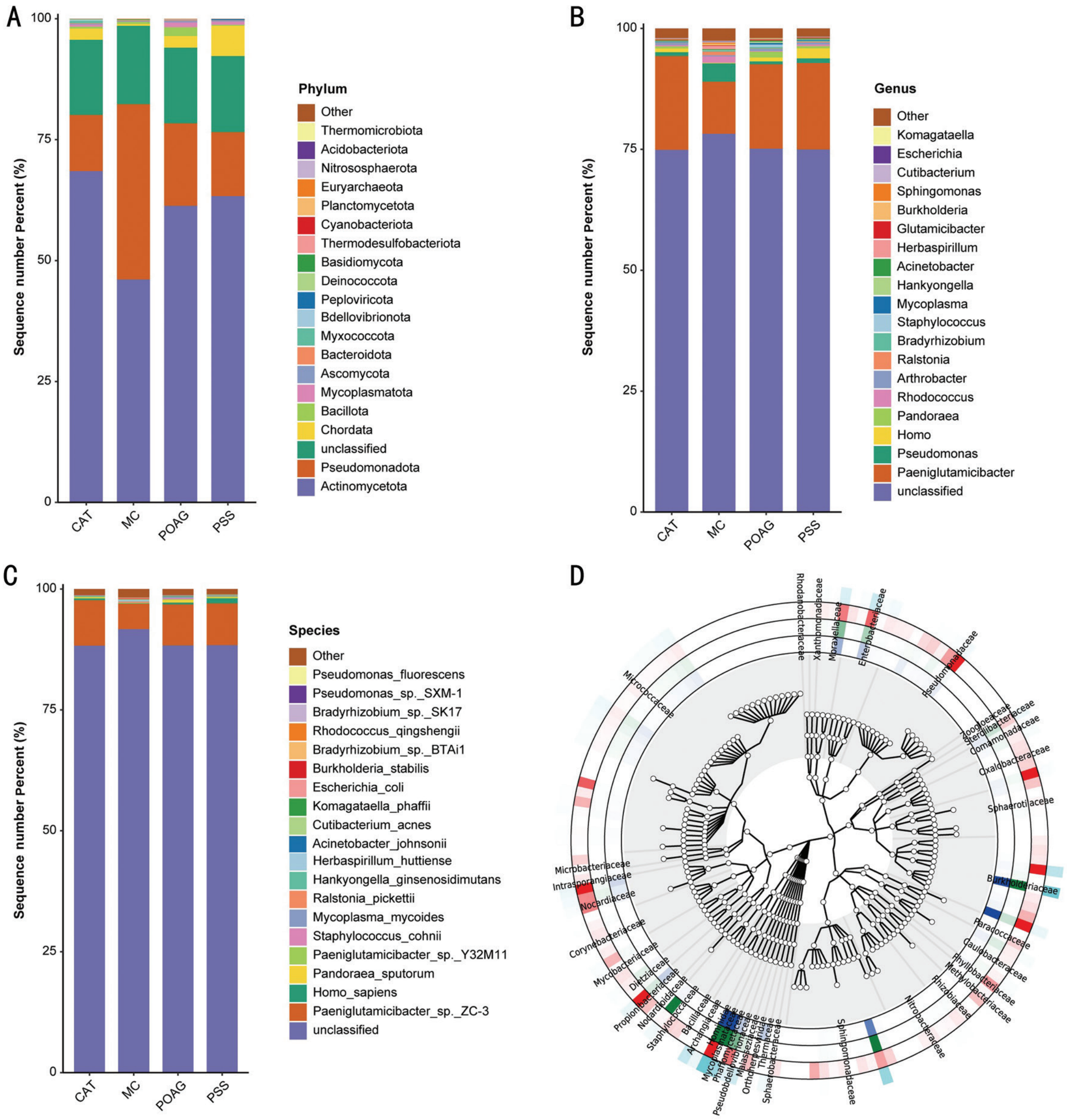

Figure 1 The composition of ocular microbiome in aqueous humor across different groups A: Relative abundance of the dominant bacterial phyla; B: Relative abundance of the dominant bacterial genera; C: Relative abundance of the dominant bacterial species; D: Phylogenetic tree based on taxonomic assignments of top 100 OTUs for the indicated phyla that were detected in the four groups. MC: Myopia control; CAT: Cataract; POAG: Primary open angle glaucoma; PSS: Posner-Schlossman syndrome; OTUs: Operational taxonomic units.

persisted for all indices (Chao1: *F*=6.459, *P*<0.001; ACE: *F*=2.764, *P*=0.049; Shannon: *F*=4.265, *P*=0.006; Richness: *F*=5.982, *P*<0.001; Table 4). Pairwise comparisons with Tukey's HSD correction (Table 5) revealed that both POAG and PSS had significantly lower Chao1 indices compared to controls (MC *vs* POAG: adjusted *P*=0.001; MC *vs* PSS: adjusted *P*=0.007), while cataract showed no significant difference after adjustment (CAT *vs* MC: adjusted *P*=0.283). Additionally, no significant differences were observed among the three disease groups themselves (*e.g.*, CAT *vs* POAG, CAT *vs* PSS, and POAG *vs* PSS, all *P*>0.05). Similar patterns were observed for Shannon and Richness indices, indicating that the reduced alpha diversity in POAG and PSS is disease-specific, while the apparent reduction in cataract might be linked to age.

Difference in the Dominant Microbiota Among Myopia Controls and Patients with Cataract, POAG, and PSS

The reduction in microbial community richness and evenness might be associated with shifts in dominant microbial populations in the aqueous humor of cataract, POAG, and PSS patients. Thus, we applied LEfSe analysis to further illustrate the difference in the dominant microbiota distribution among MCs and patients with cataract, POAG, and PSS (Figure 3A). By using LDA and Kruskal-Wallis test to detect significant differences in the abundance of OTUs among four groups, we identified that 41 species from 17 genera (such as *Cutibacterium*, *Sphingomonas*, and *Corynebacterium*) were predominant in MCs. As expected, we detected CMV as dominant microbiota in PSS groups (LDA=3.91), which was

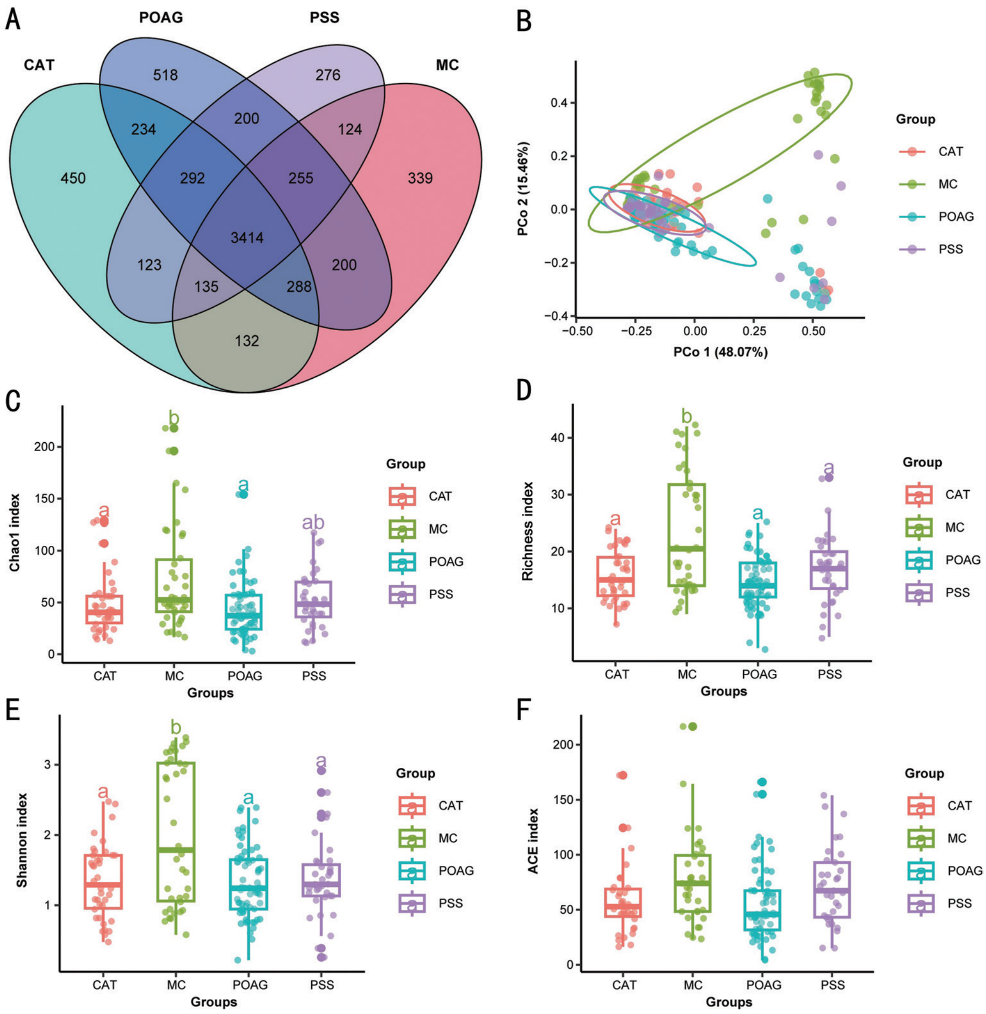

Figure 2 The comparison of microbiota diversity among myopia subjects and patients with cataract, POAG, and PSS A: Venn diagram analysis based on OTUs in the four groups; B: PCoA plot of microbial communities in the aqueous humor using Bray-Curtis distances; C: Boxplot of the Chao1 index; D: Boxplot of the Richness index; E: Boxplot of the Shannon index; F: Boxplot of the ACE index. MC: Myopia control; CAT: Cataract; POAG: Primary open angle glaucoma; PSS: Posner-Schlossman syndrome; OTUs: Operational taxonomic units; PCoA: Principal coordinate analysis; ACE: Abundance-based coverage estimator.

Table 4 ANCOVA results for alpha diversity indices

Index	*F*	*P*
Chao1		
Age	1.188	0.277
Gender	0.019	0.889
Group	6.459	<0.001
ACE		
Age	0.54	0.465
Gender	0	0.999
Group	2.764	0.049
Shannon		
Age	2.295	0.132
Gender	0.221	0.639
Group	4.265	0.006
Richness		
Age	2.627	0.107
Gender	0.181	0.671
Group	5.982	<0.001

ANCOVA: Analysis of covariance; ACE: Abundance-based coverage estimator.

reported to be the result of recurrent human CMV infection. At the genus level, we also found 11 dominant microbial taxa (such as *Paeniglutamicibacter*, *Arthrobacter*, and *Bdellovibrio*) in cataract patients and 10 dominant microbiotas (such as *Bradyrhizobium*, *Sulfuritalea*, and *Caulobacter*) in POAG patients.

To validate disease-specific taxonomic biomarkers while controlling for age, we performed LEfSe analysis on an age-matched subgroup of patients aged 35–50y (MC: *n*=5; Cataract: *n*=5; POAG: *n*=34; PSS: *n*=19; Figure 3B). As expected, the substantially reduced sample size (*n*=63 *vs* 176) limited statistical power, resulting in fewer significant features compared to the full dataset. Notably, CMV enrichment in PSS patients persisted in the age-matched analysis (LDA=3.10), consistent with its well-established role as a clinical marker independent of age. In contrast, *Paeniglutamicibacter*, which was enriched in cataract in the full analysis, did not reach significance in the age-matched subset, consistent with the

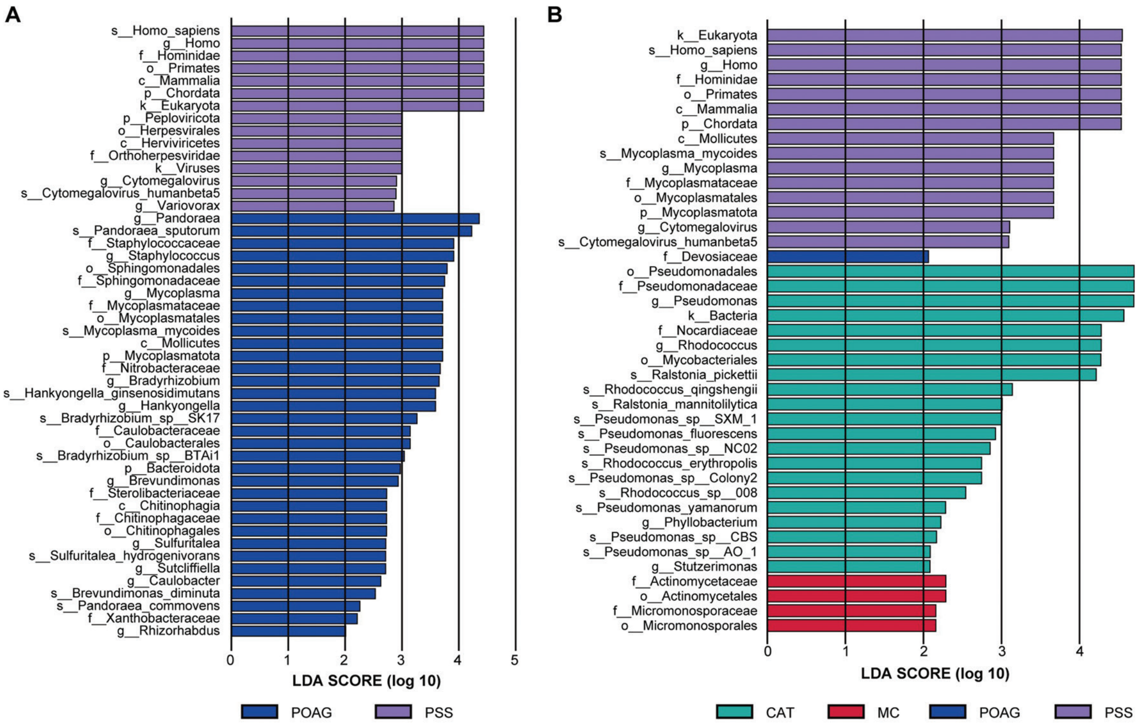

Figure 3 LEfSe analysis of microbiota distribution in aqueous humor A: Dominant microbiota of PSS and POAG patients; B: Difference analysis of microbiome among age-matched groups. MC: Myopia control; CAT: Cataract; POAG: Primary open angle glaucoma; PSS: Posner-Schlossman syndrome; LDA: Linear discriminant analysis.

Table 5 Pairwise comparisons of alpha diversity indices between groups

Index	Estimate	*P*	Adjusted *P*
Chao1			
CAT *vs* MC	-17.44	0.142	0.283
CAT *vs* POAG	5.23	0.880	0.999
CAT *vs* PSS	5.52	0.843	0.999
MC *vs* POAG	22.66	<0.001	0.001
MC *vs* PSS	22.95	0.002	0.007
POAG *vs* PSS	0.29	0.999	0.999
ACE			
CAT *vs* MC	-42.9	0.431	0.862
CAT *vs* POAG	7.94	0.991	0.998
CAT *vs* PSS	11.64	0.955	0.998
MC *vs* POAG	50.84	0.039	0.233
MC *vs* PSS	54.54	0.127	0.381
POAG *vs* PSS	3.7	0.998	0.998
Shannon			
CAT *vs* MC	-0.45	0.344	0.689
CAT *vs* POAG	0.17	0.897	1
CAT *vs* PSS	0.16	0.888	1
MC *vs* POAG	0.62	0.004	0.026
MC *vs* PSS	0.62	0.024	0.072
POAG *vs* PSS	0	1	1
Richness			
CAT *vs* MC	-2.83	0.236	0.473
CAT *vs* POAG	1.14	0.815	0.978
CAT *vs* PSS	1.26	0.737	0.978
MC *vs* POAG	3.97	<0.001	0.003
MC *vs* PSS	4.09	0.004	0.011
POAG *vs* PSS	0.12	0.999	0.999

MC: Myopia control; CAT: Cataract; POAG: Primary open angle glaucoma; PSS: Posner-Schlossman syndrome; ACE: Abundance-based coverage estimator.

interpretation that this signal was largely age-driven rather than cataract-specific. Similarly, some microbial biomarkers identified in the full dataset (such as *Cutibacterium* in controls) were also not consistently detected in the smaller subgroup, reflecting the combined effects of reduced statistical power and potential age-dependence.

Functional Features of Microbiome in Aqueous Humor To elucidate the functional potential of microbial communities in aqueous humor across different pathological states, we performed gene function annotation and pathway annotation followed by LEfSe analysis. With Gene Ontology (GO) analysis using humann3, a total of 23 763 unigenes were assigned to 1890 GO terms, revealing similar functional composition among cataract, POAG, PSS, and MCs, with high relative abundance in integral component of membrane, adenosine triphosphate (ATP) binding, cytoplasm, DNA binding, plasma membrane, and metal ion binding (Figure 4A). LEfSe analysis identified group-specific GO signatures (LDA score >2; Figure 4B), with alpha-mannosidase activity (LDA=2.11), 1-acylglycerol-3-phosphate O-acyltransferase activity (LDA=2.01), and enoyl-CoA hydratase activity (LDA=2.00) being discriminative for PSS patients, and rRNA binding (LDA=3.17), flavin adenine dinucleotide binding (LDA=2.83) and tRNA binding (LDA=2.80) markedly elevated in cataract patients. Additionally, the POAG group showed predominant enrichment in hydrolase activity (both LDA>3), beta-galactosidase activity (LDA=3.81),

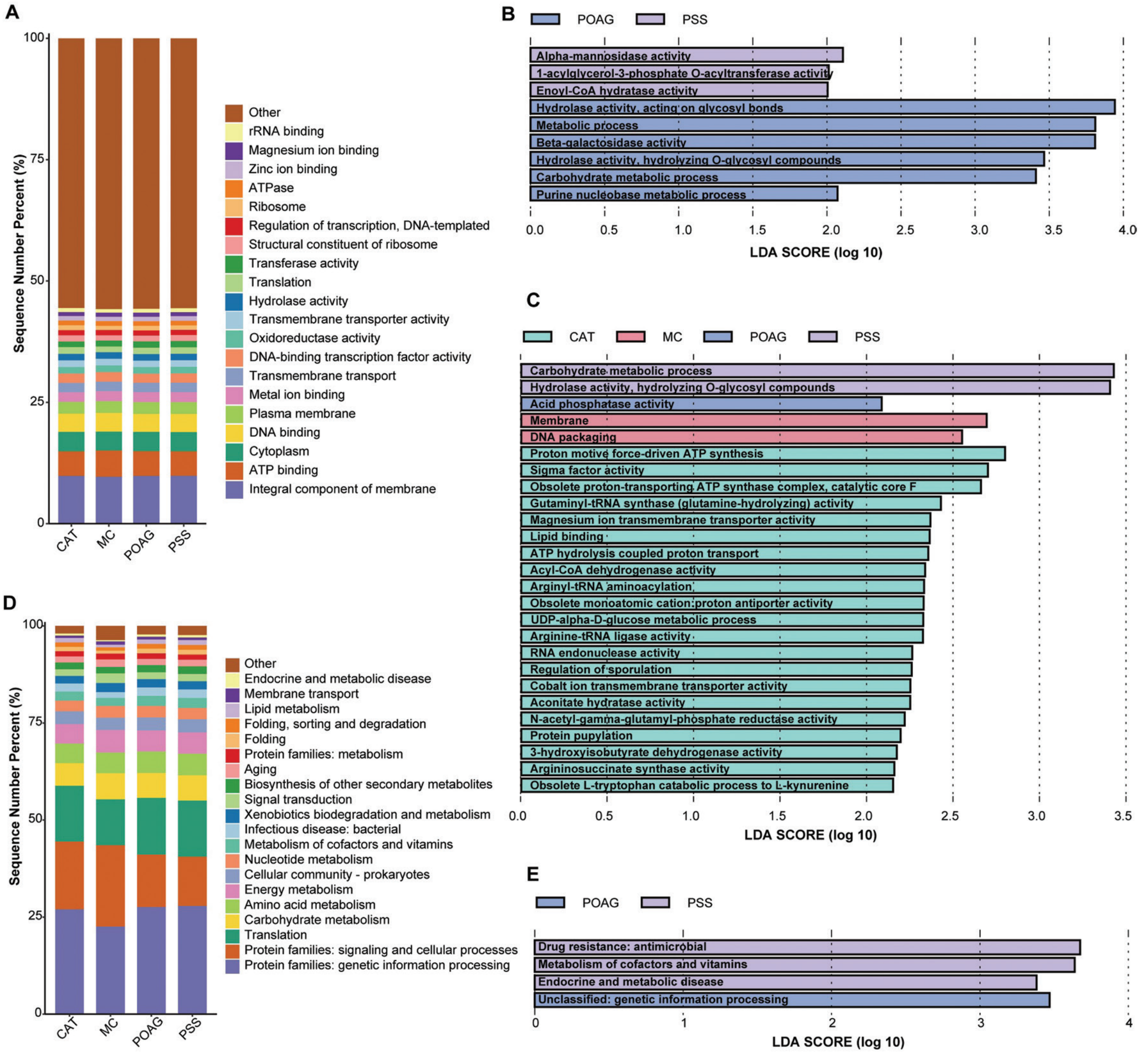

Figure 4 Functional features of microbiome in aqueous humor A: Composition of GO terms in the four groups; B: POAG-specific and PSS-specific GO terms; C: Difference analysis of GO terms among age-matched groups; D: Composition of KEGG pathways in the four groups; E: Difference analysis of KEGG metabolic pathway among four groups. MC: Myopia control; CAT: Cataract; POAG: Primary open angle glaucoma; PSS: Posner-Schlossman syndrome; LDA: Linear discriminant analysis; ATP: Adenosine triphosphate; GO: Gene Ontology; KEGG: Kyoto Encyclopedia of Genes and Genomes.

and metabolic process (including carbohydrate and purine nucleobase metabolic process, all LDA>2).

In the age-matched subgroup analysis (35–50y), several functionally consistent signals persisted despite the reduced sample size (Figure 4C). In PSS, enrichment for carbohydrate metabolic process (LDA=3.42) and hydrolase activity (LDA=3.40), hydrolyzing O-glycosyl compounds remained significant. These are broader functional categories that encompass the more specific enzyme activities detected in the full analysis, such as alpha-mannosidase activity (a glycoside hydrolase involved in carbohydrate metabolism) and enoyl-CoA hydratase activity (an enzyme participating in fatty acid oxidation, functionally linked to hydrolase activity). In POAG, acid phosphatase activity (LDA=2.08) persisted in the age-matched subset. This enzyme subclass is functionally consistent with, and indeed a specific example of, the hydrolase activity and metabolic process enrichment observed in the full dataset, and has been implicated in inflammatory responses relevant to POAG pathogenesis.

For pathway analysis, Kyoto Encyclopedia of Genes and Genomes (KEGG) pathway distribution revealed disease-associated metabolic preferences (Figure 4D and 4E). No biomarker pathways were observed in the MC group by LEfSe analysis (LDA score>2). In contrast, pathways related to drug resistance, metabolism of cofactors and vitamins, and endocrine and metabolic disease were significantly enriched in PSS patients, whereas pathways related to genetic information processing and translation were significantly enriched in cataract patients.

Correlation of Microbiome in Aqueous Humor and Metabolic Pathway and Clinical Phenotypes To investigate potential interactions between microbial communities, metabolic functions, and clinical phenotypes, we performed comprehensive correlation analyses across patients with

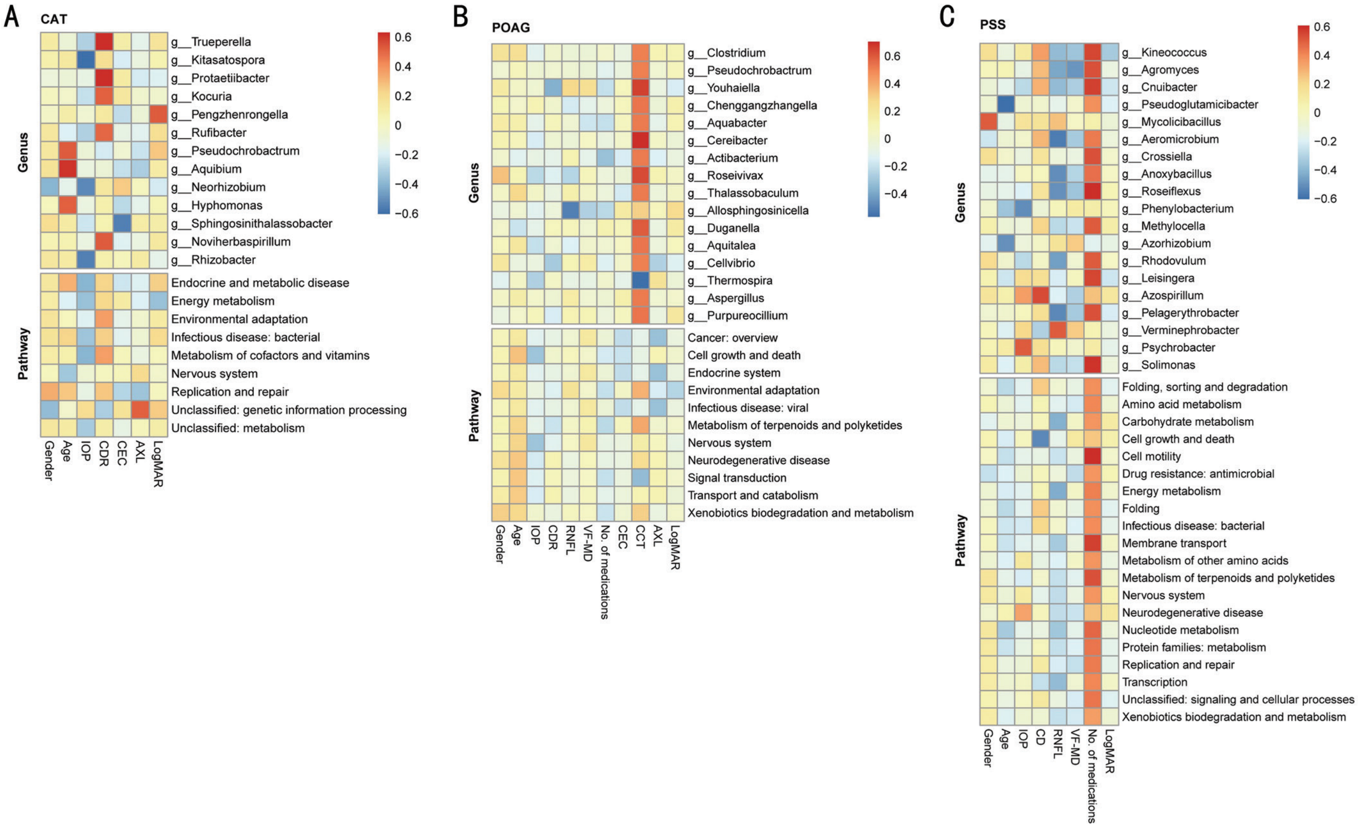

Figure 5 Correlation analysis of microbiome in aqueous humor at the genus level and KEGG pathways and clinical phenotypes A: CAT group; B: POAG group; C: PSS group. CAT: Cataract; POAG: Primary open angle glaucoma; PSS: Posner-Schlossman syndrome; logMAR: Logarithm of the minimum angle of resolution; AXL: Axial length; CCT: Central corneal thickness; CEC: Corneal endothelial cells; VF-MD: Visual field mean defect; RNFL: Retinal nerve fiber layer; CDR: Cup-disc ratio; IOP: Intraocular pressure.

cataract, POAG, and PSS (Figure 5). The age of cataract patients was significantly correlated positively with the abundance of *Pseudochrobactrum* (r=0.53, P=7.8×10^{-4}) and negatively with pathways associated with nervous system (r=-0.33, P=0.044). *Micrococcus* abundance showed positive association with axial length (AXL; r=0.45, P=5.0×10^{-3}), while *Mesorhizobium* correlated positively with IOP (r=0.54, P=5.8×10^{-4}) in the cataract group.

For POAG patients, we found that 14 genera were positively correlated with CCT (all P<0.05). Additionally, *Allosphingosinicella* displayed negative correlations with RNFL (r=-0.51, P=5.5×10^{-4}), *Youhaiella* decreased with CDR (r=-0.37, P=6.7×10^{-3}), and *Thermospira* decreased with IOP (r=-0.26, P=0.040). Pathway analysis highlighted "nervous system" and "cell growth and death"-related pathways correlating with IOP (r=-0.31 and r=-0.30, respectively, both P<0.05), suggesting a potential microbial role in disease progression.

The PSS group demonstrated unique correlation patterns. *Psychrobacter* and *Phenylobacterium* showed opposing associations with IOP (r=0.50 and r=-0.52, respectively, both P<0.01). There were eight genera displaying negative correlations with RNFL thickness and positive correlations with medication burden (all P<0.05). Strikingly, pathways related to neurodegenerative diseases were positively correlated with IOP (r=0.34, P=0.047), and the antimicrobial resistance pathway was positively correlated with medication use (r=0.38, P=0.029), possibly reflecting treatment-induced microbiome adaptation.

Moreover, sex-stratified analysis within each disease group revealed several genera with moderate effect sizes, including *Mycolicibacillus* enriched in females with PSS ($\log_2$FC=3.88, Wilcoxon P=0.003) and *Roseivivax* enriched in females with POAG ($\log_2$FC=2.09, P=0.006). However, none of these associations remained significant after FDR correction for multiple testing, underscoring the need for validation in larger cohorts.

DISCUSSION

Given the role of the microbiota in the pathogenesis of ocular diseases, a growing number of studies have revealed microbial alterations at the gut and ocular surface[24-25]. However, the intraocular environment has traditionally been considered absolutely sterile, and thus the local microbiota of the eye under physiological and pathological conditions remains largely uncharacterized. In 2021, Deng *et al*[4] presented the first evidence of the existence of an intraocular microbiota in humans. In this study, we used next-generation metagenomic sequencing to perform a comprehensive analysis of the aqueous humor microbiome in patients with cataract, POAG, and PSS, as well as in young myopia controls. Our findings suggest that the complexity and specific signatures of the intraocular microbiota may characterize different ocular disease. This unbiased approach could detect not only bacteria but also fungi and viruses, capturing more complex microbial ecosystems. Our findings are consistent with and extend previous observations regarding the existence of a low-biomass intraocular microbiome, while providing novel insights into disease-specific microbial signatures and their potential functional implications.

Several key findings emerge from our study. First, we observed distinct microbial community structures in the aqueous humor of cataract, POAG, and PSS patients compared with young myopia individuals which served as controls. The reduced alpha diversity observed in all patient groups suggests that ocular diseases may be associated with a loss of microbial homeostasis, mirroring patterns seen in other microbiome-associated disorders. This phenomenon aligns with the trend of microbial community simplification observed in various autoimmune diseases, such as rheumatoid arthritis and systemic lupus erythematosus[26-28]. Under disease conditions, the reduced diversity may reflect the suppressive effects of chronic changes in the immune microenvironment on microbial ecology, or enhanced microbial clearance due to immune dysregulation. This depletion may have significant functional consequences. By analogy from concepts of dysbiosis in autoimmune and allergic diseases, we hypothesized that the low-abundance microbiome in the healthy eye may act as an "immune calibrator"[29-30]. By providing constant exposure to microbial antigens, it could help maintain the tolerant homeostasis of the intraocular immune system. The absence of this micro-stimulation (microbial depletion) may lead to dysregulated local immune modulation, potentially rendering the eye more susceptible to exaggerated inflammatory responses against self-antigens or external triggers, thereby contributing to diseases like PSS or glaucoma.

An important observation from our adjusted analyses is the differential pattern between cataract and the other disease groups. After rigorous statistical adjustment for age and gender, both PSS and POAG retained significant differences in microbial community structure and alpha diversity compared to controls, suggesting disease-specific alterations independent of demographic factors. The persistence of CMV in PSS and carbohydrate-related metabolic pathways in PSS, as well as hydrolase-related activity in POAG, in both full and age-matched subgroup analyses further support the robustness of these disease-associated signatures. In contrast, the cataract group showed no significant differences after adjustment, and all cataract-associated signatures lost significance in the age-matched subset, suggesting that the observed microbial changes in cataract patients are largely attributable to age-related physiological processes rather than cataract pathology. This interpretation is consistent with Zhao *et al*[31], who demonstrated that age is a significant determinant of conjunctival microbiota composition in cataract patients, further underscoring the importance of age considerations in ocular microbiome studies. Furthermore, the persistence of distinct microbial community structure and reduced alpha diversity in POAG and PSS after rigorous adjustment for age and gender suggests that these conditions, both characterized by inflammatory and immune components, exhibit age-independent microbial alterations that may be involved in disease pathogenesis. However, although we employed rigorous statistical adjustments and age-matched subgroup analyses to mitigate this confound, residual confounding cannot be entirely excluded. Additionally, age-related metabolic changes including insulin resistance and low-grade inflammation are inherently linked to aging and may independently influence microbial communities[32-33]. Although we excluded patients with diagnosed diabetes and other metabolic disorders, subclinical metabolic alterations and unmeasured lifestyle factors cannot be entirely ruled out as potential confounders. Future studies with age-matched healthy controls, potentially using less invasive sampling methods or prospective cohort designs, would be valuable to further validate these findings, particularly regarding the cataract group.

In our study, we discovered not only a change in species richness and evenness but also a shift in the microbial composition of the aqueous humor microbiome. The enrichment of *Actinomycetota* in patient groups versus *Pseudomonadota* in MCs suggested potential disease-specific microbial adaptations. In line with recent studies, the existence of microbiota in the aqueous humor may suggest the microbial translocation to intraocular sites[34]. O'Keeffe *et al*[35] also reported that, in both healthy and diseased animal models, intestinal bacteria translocate into the bloodstream and many other internal organs, including the eyes, revealing that the intraocular cavity may also be inhabited by a microbial community. Our work further supports the presence of disease-associated variations in this process across different ocular diseases. Our PCoA results also demonstrate significant segregation in microbial community structure between the disease groups and the MC group, suggesting that the disease state may directly drive microbiome remodeling.

Furthermore, our LEfSe analysis revealed unique microbial biomarkers for each disease state. We identified CMV as a potential biomarker for PSS, as it was consistently enriched in this group in both the full dataset and the age-matched subgroup analysis. This finding supported the long-standing clinical associations between CMV infection and PSS[9,36-37]. For instance, Chee and Jap[38] reported a CMV-positive rate of 52.2% in eyes with presumed PSS, and Teoh *et al*[39] associated acute relapse with CMV detected by quantitative polymerase chain reaction (PCR). Furthermore, in contrast to previous studies that predominantly relied on targeted PCR assays, our metagenomic approach provided a comprehensive survey of the entire microbial community including bacteria, archaea, viruses, and eukaryotes. The rediscovery of CMV as a key driver of PSS validates the power and reliability of metagenomic sequencing in confirming and exploring the etiology of ocular infectious diseases. However, the limited sample volume from aqueous humor precluded PCR validation and precise stratification of patients based on CMV status. Future studies integrating targeted viral detection are essential to delineate the interactions between CMV, the bacterial microbiome, and clinical outcomes in PSS.

At present, the pathogenesis of POAG has not been fully elucidated. Increasing evidence suggests that glaucoma may be an immune-related disease. Guo *et al*[40] found that the proportion of Th2 and Treg cells increased in the serum of POAG patients, which further suggests the correlation between immunity and glaucomatous optic nerve damage. The enrichment of *Bradyrhizobium* in the POAG group might play a role in chronic inflammation regulation. In the stomach of patients with *Helicobacter pylori* (Hp)-positive gastritis, *Bradyrhizobium* is one of the dominant gastric bacterial genera[41]. In the meanwhile, many previous studies suggest Hp infection showed statistically significant association with POAG[42-44]. Thus, the characteristics of both gut and intraocular microbiome may be related. The mechanisms of microbial translocation and the interaction of microbiomes from different organs remain unclear; intricate cellular factors, immune cells, and pathways may be involved. Moreover, the functional pathway analysis also provided insights, with PSS showing enrichment in drug resistance pathways, which might explain the challenging clinical management of this condition. Similarly, the association between carbohydrate metabolism pathways and POAG could reflect microbial influences on trabecular meshwork function and IOP regulation.

The observed correlations between microbiota/pathway and clinical phenotype offered potential mechanistic links worth further exploration. For instance, the positive association between *Pseudochrobactrum* abundance and age in cataract patients suggested microbial involvement in lens aging. Also, the negative correlation between *Thermospira* and IOP in POAG patients suggests protective microbial functions on pressure regulation, possibly through modulation of aqueous humor outflow pathways. Interestingly, IOP showed a negative association with nervous system-related pathways in POAG and a positive association with neurodegenerative disease-related pathways in PSS, indicating the potential function of microbiota in disease progression. Additionally, the positive correlations between antimicrobial resistance pathway and medication use might inform medication strategies for PSS patients due to microbiome adaptation. Although these associations did not withstand FDR correction, they offer preliminary clues worthy of future investigation.

Our study has several limitations that warrant consideration. The cross-sectional design precludes causal inferences about microbiome-disease relationships. Given the modest sample size and the inherent challenges of low-biomass metagenomic sequencing, this study should be considered hypothesis-generating. Next, all techniques have limitations and bias, while we implemented rigorous contamination controls, the challenges of low-biomass microbiome studies persist, and our findings should be validated through independent replication. Besides, obtaining aqueous humor from completely healthy controls is inherently challenging, so we enrolled myopia patients who underwent ICL implantation surgery as controls, but alterations in the aqueous humor microbiome associated with myopic status, and particularly those that might occur in pathologic myopia, could potentially confound the results. Additionally, the functional predictions derived from metagenomic data require experimental validation to establish their biological relevance. Future studies incorporating longitudinal sampling, multi-omics approaches, and germ-free animal models could help elucidate the mechanisms underlying our observations.

Despite these limitations, our findings may have potential clinical implications. The intraocular microbiome may regulate the local immune microenvironment, a process that could involve a variety of cells, inflammatory mediators, and molecular pathways, potentially contributing to different eye diseases. The disease-specific microbial signatures we identified could serve as diagnostic biomarkers or therapeutic targets. The findings, particularly for PSS and POAG where signals were most robust, provide a foundation for future targeted investigations with larger sample sizes and age-matched controls. For example, the CMV signature in PSS supports existing antiviral treatment approaches, while the unique bacterial profiles in POAG may inform novel probiotic or antibiotic strategies. Furthermore, the functional pathway differences suggest opportunities for metabolic interventions in ocular diseases.

ACKNOWLEDGEMENTS

Authors' Contributions: Zhang C conceived and designed the

study; Hong J, Zhang C, Wang HZ and Zhang Y provided the resources; Zhang WJ, Wu HL, Xia ZY, Zhang D, Suo LG and Pan Z collected the clinical data and aqueous humor samples; Yang Z and She JQ analyzed the data; Yang Z and Zhang WJ interpreted the data and wrote the manuscript. All authors approved the final version of the manuscript.

Data Availability Statement: The datasets supporting the conclusions of this article are available in the NCBI SRA repository (PRJNA1187273), https://submit.ncbi.nlm.nih.gov/subs/bioproject/SUB14872365/overview.

Foundation: Supported by the Beijing Municipal Science and Technology Plan Project (No.Z241100009024040).

Conflicts of Interest: Zhang WJ, None; **Yang Z,** None; **She JQ,** None; **Wu HL,** None; **Xia ZY,** None; **Zhang D,** None; **Suo LG,** None; **Pan Z,** None; **Zhang Y,** None; **Wang HZ,** None; **Hong J,** None; **Zhang C,** None.

REFERENCES

1 Aggarwal N, Kitano S, Puah GRY, *et al*. Microbiome and human health: current understanding, engineering, and enabling technologies. *Chem Rev* 2023;123(1):31-72.

2 Ma ZQ, Zuo T, Frey N, *et al*. A systematic framework for understanding the microbiome in human health and disease: from basic principles to clinical translation. *Signal Transduct Target Ther* 2024;9(1):237.

3 Wen XF, Hu X, Miao L, *et al*. Epigenetics, microbiota, and intraocular inflammation: New paradigms of immune regulation in the eye. *Prog Retin Eye Res* 2018;64:84-95.

4 Deng Y, Ge X, Li Y, *et al*. Identification of an intraocular microbiota. *Cell Discov* 2021;7(1):13.

5 Artero-Castro A, Rodriguez-Jimenez FJ, Jendelova P, *et al*. Glaucoma as a neurodegenerative disease caused by intrinsic vulnerability factors. *Prog Neurobiol* 2020;193:101817.

6 Yang X, Li S, Guo H, *et al*. Emerging roles of the immune microenvironment in glaucoma. *Clin Exp Optom* 2026;109(4):572-578.

7 Zhang DW, Wu JW, Zhang SH, *et al*. Identification of immune infiltration-related ceRNAs as novel biomarkers for prognosis of patients with primary open-angle glaucoma. *Front Genet* 2022;13:838220.

8 Zavos C, Kountouras J, Sakkias G, *et al*. Histological presence of *Helicobacter pylori* bacteria in the trabeculum and iris of patients with primary open-angle glaucoma. *Ophthalmic Res* 2012;47(3):150-156.

9 Lee SH, Ho YR, Li H, *et al*. Prevalence and clinical manifestations of cytomegalovirus infection in patients with Posner-Schlossman syndrome: a systematic review and meta-analysis. *Surv Ophthalmol* 2025;70(6):1252-1260.

10 Consortium M, Qin JJ, Li RQ, *et al*. A human gut microbial gene catalogue established by metagenomic sequencing. *Nature* 2010;464(7285):59-65.

11 Quince C, Walker AW, Simpson JT, *et al*. Shotgun metagenomics, from sampling to analysis. *Nat Biotechnol* 2017;35(9):833-844.

12 Kelly BJ, Gross R, Bittinger K, *et al*. Power and sample-size estimation for microbiome studies using pairwise distances and PERMANOVA. *Bioinformatics* 2015;31(15):2461-2468.

13 Prast-Nielsen S, Tobin AM, Adamzik K, *et al*. Investigation of the skin microbiome: swabs *vs*. biopsies. *Br J Dermatol* 2019;181(3):572-579.

14 Herzog EL, Kreuzer M, Zinkernagel MS, *et al*. Challenges and insights in the exploration of the low abundance human ocular surface microbiome. *Front Cell Infect Microbiol* 2023;13:1232147.

15 Shen JX, McFarland AG, Blaustein RA, *et al*. An improved workflow for accurate and robust healthcare environmental surveillance using metagenomics. *Microbiome* 2022;10(1):206.

16 Bai DF, Chen T, Xun JN, *et al*. EasyMetagenome: a user-friendly and flexible pipeline for shotgun metagenomic analysis in microbiome research. *Imeta* 2025;4(1):e70001.

17 Chen SF. Ultrafast one-pass FASTQ data preprocessing, quality control, and deduplication using fastp. *Imeta* 2023;2(2):e107.

18 Langmead B, Salzberg SL. Fast gapped-read alignment with bowtie 2. *Nat Methods* 2012;9(4):357-359.

19 Lu J, Rincon N, Wood DE, *et al*. Metagenome analysis using the Kraken software suite. *Nat Protoc* 2022;17(12):2815-2839.

20 Lu J, Breitwieser FP, Thielen P, *et al*. Bracken: estimating species abundance in metagenomics data. *Peerj Comput Sci* 2017;3:e104.

21 Beghini F, McIver LJ, Blanco-Míguez A, *et al*. Integrating taxonomic, functional, and strain-level profiling of diverse microbial communities with bioBakery 3. *Elife* 2021;10:e65088.

22 Segata N, Izard J, Waldron L, *et al*. Metagenomic biomarker discovery and explanation. *Genome Biol* 2011;12(6):R60.

23 Liu YX, Chen L, Ma TF, *et al*. EasyAmplicon: an easy-to-use, open-source, reproducible, and community-based pipeline for amplicon data analysis in microbiome research. *Imeta* 2023;2(1):e83.

24 Xue W, Li JJ, Zou YL, *et al*. Microbiota and ocular diseases. *Front Cell Infect Microbiol* 2021;11:759333.

25 Napolitano P, Filippelli M, Davinelli S, *et al*. Influence of gut microbiota on eye diseases: an overview. *Ann Med* 2021;53(1):750-761.

26 Tsetseri MN, Silman AJ, Keene DJ, *et al*. The role of the microbiome in rheumatoid arthritis: a review. *Rheumatol Adv Pract* 2023;7(2):rkad034.

27 Belizário JE, Napolitano M. Human microbiomes and their roles in dysbiosis, common diseases, and novel therapeutic approaches. *Front Microbiol* 2015;6:1050.

28 Bäckhed F, Fraser CM, Ringel Y, *et al*. Defining a healthy human gut microbiome: current concepts, future directions, and clinical applications. *Cell Host Microbe* 2012;12(5):611-622.

29 Lawton R. Early-life infectious disease exposure, the “hygiene hypothesis,” and lifespan: Evidence from hookworm disease. *Proc Natl Acad Sci U S A* 2025;122(35):e2504265122.

30 Perkin MR, Strachan DP. The hygiene hypothesis for allergy–conception and evolution. *Front Allergy* 2022;3:1051368.

31 Zhao TY, Sun YJ, Wang JY, *et al*. Conjunctival microbiota variations in a subset of middle-aged and elderly individuals from Beijing, China. *Int J Ophthalmol* 2025;18(2):237-243.

32 Semo D, Reinecke H, Godfrey R. Gut microbiome regulates inflammation and insulin resistance: a novel therapeutic target to improve insulin sensitivity. *Signal Transduct Target Ther* 2024;9(1):35.

33 Shintouo CM, Mets T, Beckwee D, *et al*. Is inflammageing influenced by the microbiota in the aged gut? A systematic review. *Exp Gerontol* 2020;141:111079.

34 Li JJ, Yi SJ, Wei L. Ocular microbiota and intraocular inflammation. *Front Immunol* 2020;11:609765.

35 O'Keeffe KM, Wilk MM, Leech JM, *et al*. Manipulation of autophagy in phagocytes facilitates staphylococcus aureus bloodstream infection. *Infect Immun* 2015;83(9):3445-3457.

36 Liu H, Lai YX, Liu YN, *et al*. Clinical characteristics of viral-associated Fuchs uveitis syndrome and Posner-Schlossman syndrome in a Chinese population. *Graefes Arch Clin Exp Ophthalmol* 2024;262(10):3305-3312.

37 Megaw R, Agarwal PK. Posner-schlossman syndrome. *Surv Ophthalmol* 2017;62(3):277-285.

38 Chee SP, Jap A. Presumed fuchs heterochromic iridocyclitis and posner-schlossman syndrome: comparison of cytomegalovirus-positive and negative eyes. *Am J Ophthalmol* 2008;146(6):883-889.e1.

39 Teoh SB, Thean L, Koay E. Cytomegalovirus in aetiology of Posner–Schlossman syndrome: evidence from quantitative polymerase chain reaction. *Eye (Lond)* 2005;19(12):1338-1340.

40 Guo CY, Wu NB, Niu XY, *et al*. Comparison of T helper cell patterns in primary open-angle glaucoma and normal-pressure glaucoma. *Med Sci Monit* 2018;24:1988-1996.

41 Hua ZL, Xu L, Zhu JH, *et al*. *Helicobacter pylori* infection altered gastric microbiota in patients with chronic gastritis. *Front Cell Infect Microbiol* 2023;13:1221433.

42 Ezzati Amini E, Moradi Y. Association between helicobacter pylori infection and primary open-angle glaucoma: a systematic review and meta-analysis. *BMC Ophthalmol* 2023;23(1):374.

43 Zeng J, Liu HH, Liu X, *et al*. The relationship Between*Helicobacter pylori*Infection and open-angle glaucoma: a meta-analysis. *Invest Ophthalmol Vis Sci* 2015;56(9):5238-5245.

44 Kountouras J, Zavos C, Chatzopoulos D. *Helicobacter pylori* and glaucoma. *Ophthalmology* 2003;110(12):2433-2434.